

Corner detection in color images by multiscale combination of end-stopped cortical cells

Rolf P. Würtz¹ and Tino Lourens²

¹ Institute for Neurocomputing, Ruhr-University of Bochum, Germany

² Computing Science, University of Groningen, The Netherlands

Abstract. We present a corner-detection algorithm based on a model for end-stopping cells in the visual cortex. Shortcomings of this model are overcome by a combination over several scales. The notion of an end-stopped cell and the resulting corner detector is generalized to color channels in a biologically plausible way. The resulting corner detection method yields good results in the presence of high frequency texture, noise, varying contrast, and rounded corners. This compares favorably with known corner detectors.

1 Introduction

Corners are important image features because they are robust with respect to changes in perspective and small distortions, and they allow efficient matching for recognition purposes. It is known that removing the corners from images impedes human recognition performance, while removing much of the edge information does not [1]. Robustness and speed of corner matching can be improved by adding attributes to the corners [8]. This makes computationally expensive detection algorithms attractive, which usually yield a variety of further information.

We followed known models for the early stages of vision and checked the performance of models for end-stopped (corner detecting) cells. This compared poorly with the capabilities of the human visual system, especially in the presence of background texture and noise. The major problem was that those models act on a single scale only, whereas a robust system must check for corners on a range of scales.

2 End-stopped cells

The usual view of early vision is hierarchical processing: Retinal cells feed their output to the LGN, whose output is combined to form orientation selective simple cells. Pairs of them feed their output to complex cells, which constitute the input to end-stopped cells. The basic operations are only summation of outputs and simple nonlinearities, so this can be readily implemented by a feedforward neural network. Notwithstanding the good functional models this view provides for static images, it is far from clear that the anatomy should indeed be so simple.

The responses of even (line-enhancing) and odd (edge-enhancing) simple cells are modeled as the real and imaginary parts of the well-known Gabor functions with a DC correction (see, e.g., [5]). Complex cells are built using the *modulus* of the corresponding complex number, and we write a layer of them as $\mathcal{C}_{\sigma,\theta}(x, y)$, where σ stands for the size, θ for the orientation of the receptive field.

Cells that do respond only to those edges or bars that *terminate* within their receptive field have first been found by [4]. Two types are distinguished: the *single end-stopped cells* respond well to line-ends; the *double end-stopped cells* respond best to very short line-segments or small spots, circular objects or blobs. We follow the model of [3] and use the responses of complex cells as input for the end-stopped cells. The first step towards an end-stopped operator is an approximation of the first derivative of the \mathcal{C} -operator in the direction orthogonal to the one of the line segment in question (abbreviations $c = \cos \theta$, $s = \sin \theta$ have been used):

$$\widehat{\mathcal{S}}_{\sigma,\theta}(x, y) = \mathcal{C}_{\sigma,\theta}(x + d\sigma s, y - d\sigma c) - \mathcal{C}_{\sigma,\theta}(x - d\sigma s, y + d\sigma c). \quad (1)$$

The operator which models the receptive field functionality of double end-stopped cells approximates the second derivative of the \mathcal{C} -operator:

$$\widehat{\mathcal{D}}_{\sigma,\theta}(x, y) = \mathcal{C}_{\sigma,\theta}(x, y) - \frac{1}{2}\mathcal{C}_{\sigma,\theta}(x + 2d\sigma s, y - 2d\sigma c) - \frac{1}{2}\mathcal{C}_{\sigma,\theta}(x - 2d\sigma s, y + 2d\sigma c). \quad (2)$$

The value of d is of great importance for the functioning of the model. If it is too large, the line segment (or edge) will be eliminated in the middle and two shorter line segments will remain instead of the end points. When d is chosen too small a corner will be detected at the wrong position. We have found that the choice of $d = 1.8$ constitutes a reasonable compromise.

Parameters of the model have been adjusted using a test image where the *correct corners* have been marked manually. Every response of the modeled end-stopped cells other than at these corners is a *false response* and must be eliminated by further machinery. This is done by a tangential and a radial inhibiting operator, which are defined as follows:

$$\mathcal{I}_{\sigma}^t(x, y) = \sum_{i=0}^{2N-1} [-w_t \mathcal{C}_{\sigma,\theta_{i \bmod N}}(x, y) + \mathcal{C}_{\sigma,\theta_{i \bmod N}}(x + d\sigma c_i, y + d\sigma s_i)]^{\geq 0} \quad (3)$$

$$\mathcal{I}_{\sigma}^r(x, y) = \sum_{i=0}^{2N-1} \left[\mathcal{C}_{\sigma,\theta_{i \bmod N}}(x, y) - w_r \mathcal{C}_{\sigma,\theta_{(i + \frac{N}{2}) \bmod N}}(x + \frac{1}{2}d\sigma c_i, y + \frac{1}{2}d\sigma s_i) \right]^{\geq 0} \quad (4)$$

where $[f]^{\geq 0}$ is equal to 0 where its argument f is negative and equal to f elsewhere (halfwave rectification). N is the number of orientation samples, $\theta_i = \frac{i\pi}{N}$. $w_t = 1$ and $w_r = 4$ are positive constants, whose values have been found empirically, and work well for many input images and reasonable values of $N \in \{8, 16\}$ and $\sigma \in [1.0, 10.0]$. The final corner operators on a single scale in a single direction then are:

$$\mathcal{X}_{\sigma,\theta} = \left[\left[\widehat{\mathcal{X}}_{\sigma,\theta} \right]^{\geq 0} - g(\mathcal{I}_{\sigma}^t + \mathcal{I}_{\sigma}^r) \right]^{\geq 0}, \quad (5)$$

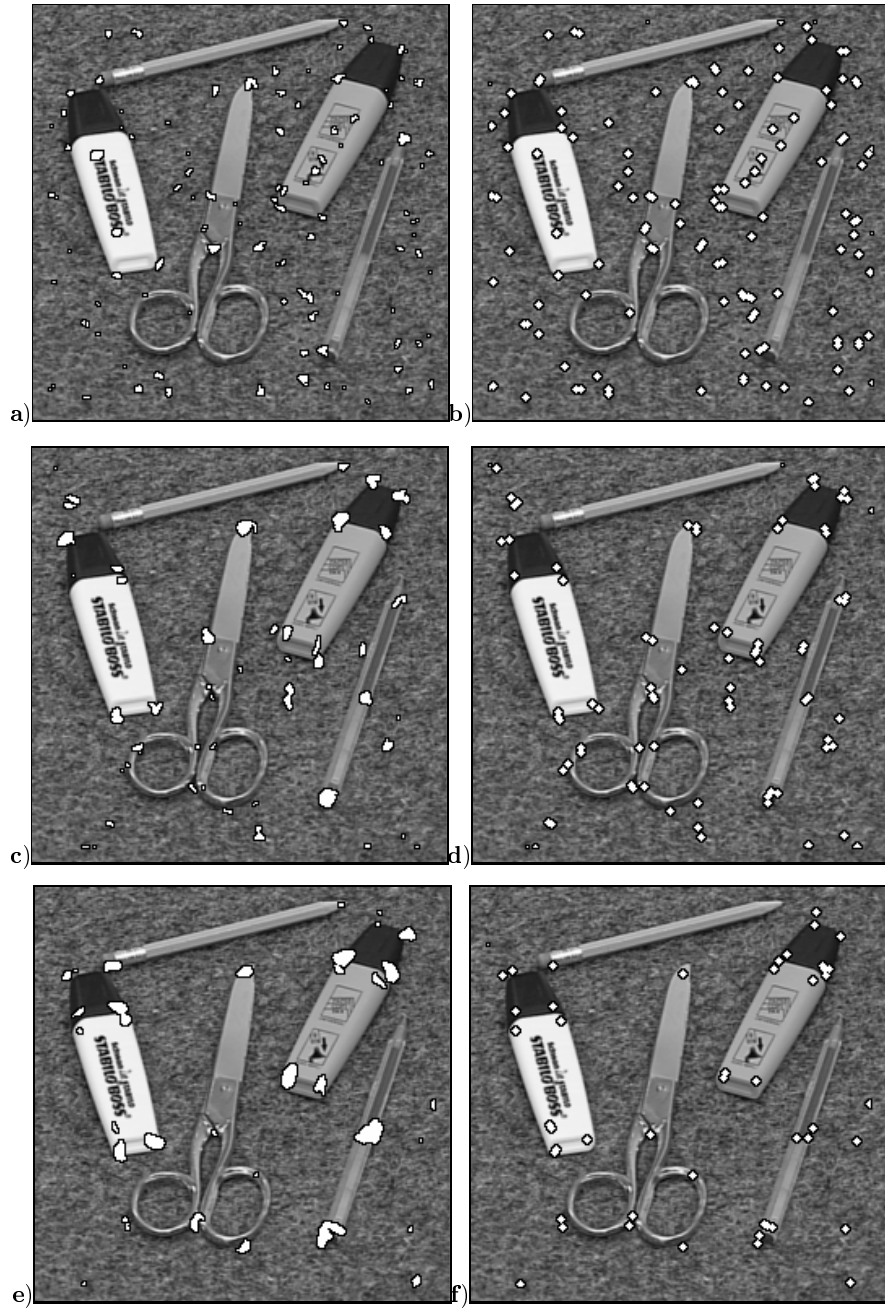


Fig. 1. The left column shows potential corner features (PCF) using receptive field sizes of $\sigma = 3.53$, $\sigma = 5.88$, and $\sigma = 8.24$, the right column the corresponding marked corners (MC). The number of orientations was $N = 8$, the image resolution 256×256 .

where \mathcal{X} stands for \mathcal{S} or \mathcal{D} and $g = 2$ is an orientation- and scale-independent gain factor.

For brevity, we here only consider the *position* of corners, ignoring further information about the orientation of the line ends and also the type of end-stopped cell that gave rise to the corner. For applications, this useful information can, of course, be kept. The resulting operator is:

$$\mathcal{E}_\sigma = \max_{i=0, \dots, 2N-1} (\max(\mathcal{S}_{\sigma, \theta_i}, \mathcal{D}_{\sigma, \theta_i})) . \quad (6)$$

In order to extract single pixels as corner points \mathcal{E}_σ has been thresholded at each scale with a fixed threshold T , which has been set to 5 for all simulations (image values range from 0 to 255). This yields little patches which we call *potential corner features (PCF)*. These patches are thinned out by taking local maxima, i.e. a point (x, y) is a *marked corner (MC)* if it is a PCF and the value \mathcal{E}_σ is larger than the ones at the neighboring pixels.

The results of the corner operator \mathcal{E}_σ on a natural image are shown in Figure 1. That image poses a difficult test-case for corner detection, it has a “noisy” background and some corners are rounded, vague, or have low contrast.

3 Combination over a range of scales

The \mathcal{E}_σ -operators at small scales locate corners very well but are very sensitive to local changes (high frequency noise) and therefore less reliable. The large scales yield only imprecise information about the corner location. We have checked the scale-dependency of location and strength of the corner operators. We found with several test images that the location on a smaller scale fell inside the PCF on larger scales and that the strength of clean corners varied by no more than 20% over the scales. This shows that the combination can be done at single locations and with equal weighting of all scales.

We have experimented with several sampling schemes for σ (linear, exponential) and different combination operators (maximum, different weighted sums, sums of powers) and found that the *average* of uniformly sampled scales gave the best results:

$$\mathcal{E}_{avg}(x, y) = \frac{1}{S} \sum_{i=0}^{S-1} \mathcal{E}_{\sigma_i}(x, y), \quad \sigma_i = \sigma_{min} + i \cdot \frac{\sigma_{max} - \sigma_{min}}{S - 1} \quad (7)$$

The marked corners that result from this operator are shown in Figure 2. They are clearly better than the ones on a single scale (right column of Figure 1).

4 Extension to color channels

The corner detection described so far as well as most corner detectors from the literature act on grey-level images. In this section we describe a biologically motivated extension to color channels. *Opponent* color-sensitive cells are found



Fig. 2. Detected corners in a variety of natural images. **a)** to **c)** show corners found in the grey-level image, **d)** the ones in the color image corresponding to **c)**. The parameter values for these results have been $N = 8$, $\sigma_{min} = 1.18$, $\sigma_{max} = 9.43$, $S = 15$.

at the first levels of processing after the photo receptors. Some of them are orientation selective and have an elongated area which is *excited* by one color, and one or two flanks which are *inhibited* by the opposite color with color pairs blue-yellow, and red-green or vice versa [6]. In area V4, color and orientation selective cells have been found [9].

A pair of such cells with opposite color pair can be combined to the equivalent of a simple cell for the color pair in question. These cells have not been found yet, but it is quite plausible that they should exist. We call them *double opponent simple cells*. Their functionality can be combined just like the one of the (grey-scale) simple cells by taking the root of the sum of squares of a pair of even and odd cells. This results in *double opponent complex cells*. Their existence has not

been shown experimentally but the repetition of the construction of the black-white pathway seems plausible. As in section 2, their outputs can be combined to form *double opponent end-stopped cells* and color-sensitive multiscale corner detectors. Although such cells have not been observed yet, they are functionally useful. Figure 2c and d show an example where the combination of red-green, blue-yellow, and greylevel channels gives better results than the greylevel channel alone.

5 Discussion

We compared the single-scale corner detection with five standard corner detection operators. On single scales they were all inferior to \mathcal{E}_σ , which is not very surprising given the higher computational cost of our approach. After scale combination, only the Plessey feature point operator [2] yielded comparable results. The high reliability of the corner detection used here made it possible to use it for the construction of a symbolic representation of objects as edge graphs [7]. Finally, we have hypothesized that end-stopped cells can also be found in color-sensitive areas, presented a functional model and shown that it is useful for corner detection.

References

1. I. Biedermann. Recognition-by-components: A theory of human image understanding. *Psychological Review*, 94(2):115–147, 1987.
2. C. Harris and M. Stephens. A combined corner and edge detector. In *Proceedings of the 4th Alvey Vis. Conf.*, pages 189–192, Manchester, August 1988.
3. F. Heitger, L. Rosenthaler, R. von der Heydt, E. Peterhans, and O. Kübler. Simulation of neural contour mechanisms: from simple to end-stopped cells. *Vision Research*, 32(5):963–981, 1992.
4. D. H. Hubel and T. N. Wiesel. Receptive fields and functional architecture in two nonstriate visual areas (18 and 19) of the cat. *Journal of Neurophysiology*, 28:229–289, March 1965.
5. T. S. Lee. Image representation using 2D Gabor wavelets. *IEEE Transactions on Pattern Analysis and Machine Intelligence*, 18(10), 1996.
6. M. S. Livingstone and D. H. Hubel. Anatomy and physiology of a color system in the primate visual cortex. *J. Neurosci.*, 4:309–356, 1984.
7. T. Lourens and R. P. Würtz. Object recognition by matching symbolic edge graphs. In *Proceedings of the Third Asian Conference on Computer Vision, Hong Kong, January 8 - 11, 1998*, 1998. In press.
8. P. L. Rosin. Augmenting corner descriptors. *Graphical Models and Image Processing*, 58(3):286–294, May 1996.
9. S. Zeki. *A Vision of the Brain*. Blackwell science Ltd., London, 1993.